COMMUNICATIONS IN COMPUTATIONAL PHYSICS
Vol. **4**, No. 4, pp. 820-837

Commun. Comput. Phys.
October 2008

# New Finite-Volume Relaxation Methods for the Third-Order Differential Equations

Fayssal Benkhaldoun[1,2] and Mohammed Seaïd[3,*]

[1] *CMLA, ENS Cachan, 61 avenue du Pdt Wison, 94 235 Cachan, France.*
[2] *LAGA, Université Paris* 13, 99 *Av J.B. Clement*, 93430 *Villetaneuse, France.*
[3] *School of Engineering, University of Durham, South Road, Durham DH1 3LE, UK.*

Received 21 November 2007; Accepted (in revised version) 17 April 2008

Communicated by Chi-Wang Shu

Available online 28 May 2008

**Abstract.** We propose a new method for numerical solution of the third-order differential equations. The key idea is to use relaxation approximation to transform the nonlinear third-order differential equation to a semilinear second-order differential system with a source term and a relaxation parameter. The relaxation system has linear characteristic variables and can be numerically solved without relying on Riemann problem solvers or linear iterations. A non-oscillatory finite volume method for the relaxation system is developed. The method is uniformly accurate for all relaxation rates. Numerical results are shown for some nonlinear problems such as the Korteweg-de Vires equation. Our method demonstrated the capability of accurately capturing soliton wave phenomena.

**AMS subject classifications**: 5L30, 76M12, 35Q53

**Key words**: Third-order differential equations, relaxation approximation, finite volume method, Korteweg-de Vries equation, solitons.

## 1 Introduction

Most work on relaxation methods is concerned with hyperbolic equations of conservation laws; there has been active research on relaxation methods for first-order differential problems (see, e.g., [3, 10, 16–18] and references therein). However, to the best of our knowledge, there is no reference in the literature on relaxation methods for dispersive,

*Corresponding author. *Email addresses:* `fayssal@math.univ-paris13.fr` (F. Benkhaldoun), `m.seaid@durham.ac.uk` (M. Seaïd)

 

namely, third and higher-order differential equations. Therefore, our goal in the present work is to develop a relaxation method for solving the third-order differential equations

$$\begin{aligned} &U_t+F(U)_x+\nu U_{xxx}=0, \qquad (x,t)\in\mathbb{R}\times\mathbb{R}^+, \\ &U(x,0)=\bar{U}(x), \qquad x\in\mathbb{R}, \end{aligned} \tag{1.1}$$

where $U(x,t)$ is the unknown solution, $F(U)$ is an arbitrary (smooth) function, $\nu$ is the dispersive coefficient and $\bar{U}(x)$ is a given initial data. The subscript $t$ and $x$ denote derivatives with respect to time and space, respectively. Eq. (1.1) arise in the modeling of many physical phenomena such as surface water waves, plasma waves, Rossby waves and harmonic lattices among others. In particular, the Korteweg-de Vires (KdV) equation has serve as a prototype for the third-order differential equations (1.1). The KdV equation is a special case of (1.1) for the choice $F(U)=U^2$ and the KdV equation is also a generic model for the study of weakly nonlinear long waves. For a comprehensive overview of the analysis and applications of the KdV equation we refer the reader to [7,9] and further references can be found therein.

It is well-known that the numerical solution of Eq. (1.1) is not trivial and many available numerical methods fail to accurately solve the problem under consideration. Most of the numerical difficulties on solving Eq. (1.1) are associated with the nonlinear structure of the flux function $F(U)$ and the presence of the dispersive term $\nu U_{xxx}$. For example, in many applications such as in quantum hydrodynamic models or semiconductor device simulations and in the dispersive limit of conservation laws, the third-order derivative term might has small or even zero coefficients in some parts of the domain. These physical situations represent a challenge in most of computational algorithms designed for equations of conservation laws. It has long been known that conservative discretization schemes for nonlinear and non-dissipative partial differential equations governing wave phenomena tend to become numerically unstable, and dissipation has subsequently been routinely introduced into such numerical schemes.

In the last years, relaxation methods for hyperbolic partial differential equations have been subject of several investigations. We should point out that, relaxation methods were first developed in [10] for the conservation laws containing first-order derivatives. Recently, relaxation schemes have been used for gas dynamics [17], shallow water equations [18], traffic flows [16] and Hamilton-Jacobi equations [2], among other applications. The central idea in these methods is that the nonlinear conservation laws are replaced by a semilinear hyperbolic system with linear characteristics and a relaxation parameter controlling the rate of convergence to the original conservation laws [10]. The main advantage in considering relaxation methods is that Riemann solvers are completely avoided in their reconstruction. Issues of diagonalization of the so-called relaxing system, choice of approximations of the global or local characteristic speeds have been discussed in the above mentioned references.

The aim of this paper is to propose a suitable scheme to approximate numerical solution to the problem (1.1) by relaxation method such that it can be implemented efficiently

and has a good convergence property as in the case of the relaxation schemes for first-order differential equations. Numerically, the main advantage of solving the relaxation system over the original partial differential equation (1.1) lies essentially in the simple linear structure of characteristics fields and in the fact that the lower-order term is localized. In particular, the semilinear nature in the system allows for a new manner to develop numerical schemes that are simple and Riemann solver free whereas, the absence of the third-order differential term in the system eliminates the difficulties associated with boundary conditions such that the classical three-point stencil can be used. An additional advantage of the relaxation method for Eq. (1.1) is its ability to capture the wave behavior easily using simple stable discretizations. This property is crucial for the implementation of finite volume method in this work. We should point out that relaxation methods for second-order differential equations such as degenerate diffusion problems have been studied in [6, 14] among others.

The rest of the paper is organized as follows. In Section 2 we discuss the relaxation approximation of Eq. (1.1). Section 3 describes the finite volume discretization of the relaxation system. Numerical examples are presented in Section 4 to confirm the capability of this method for capturing soliton wave phenomena and various boundary wave patterns. We end the paper with a few concluding remarks in Section 5.

## 2 The relaxation approximation

The original relaxation method was designed in [10] to solve first-order hyperbolic problems. Recently, this method has been applied to a wide class of multi-dimensional partial differential equations of first and second order, see for example [2, 16–18]. In the current work we propose the following relaxation approximation of the third-order differential equations (1.1)

$$\begin{aligned} &U_t+V_x=0,\\ &V_t+AU_x=-\frac{1}{\varepsilon}\Big(V-F(U)-\nu U_{xx}\Big),\\ &U(x,0)=\bar{U},\quad V(x,0)=F\big(\bar{U}\big)+\nu\bar{U}_{xx}, \end{aligned} \tag{2.1}$$

where $V\in\mathbb{R}$ is the relaxation variable, $\varepsilon\in[0,1)$ is the parameter that measures the relaxation rate, and $A$ is the characteristic speed. Formally, as $\varepsilon\to 0$, one can recover the nonlinear dispersive equation (1.1) by projecting $V$ to the local equilibrium

$$V=F(U)+\nu U_{xx}. \tag{2.2}$$

The convergence of (2.1) to (1.1) is guaranteed if the so-called *subcharacteristic* condition [3, 10]

$$A-F'(U)^2\geq 0, \tag{2.3}$$

holds in the relaxation system (2.1) for all $U$. The condition (2.3) ensures that a numerical method for the original equation (1.1) and the relaxation system (2.1) shares the same asymptotic behavior for small values of the relaxation rate $\varepsilon$.

**Remark 2.1.** It should be stressed that the choice of relaxation approximations to Eq. (1.1) is not unique. Other types of relaxation systems which relax at the limit ($\varepsilon\to 0$) to Eq. (1.1) are also possible. For instance a three-speed relaxation system reads

$$\begin{aligned}
&U_t+V_x=0,\\
&V_t+\frac{\nu}{\varepsilon}W_x=-\frac{1}{\varepsilon}\Big(V-F(U)\Big),\\
&W_t+AU_x=-\frac{1}{\varepsilon}\Big(W-U_{xx}\Big),\\
&U(x,0)=\bar{U},\quad V(x,0)=F\big(\bar{U}\big),\quad W(x,0)=\nu\bar{U}_{xx}.
\end{aligned}\tag{2.4}$$

We point out that numerical schemes that work for the relaxation system with source term (2.1) would not apply to the system (2.4) since here, in addition to the stiff low-order term, the convective term is also stiff. Therefore, a special attention must be given to ensure that the schemes possess the correct zero relaxation, in the sense that the asymptotic limit that leads from system (2.4) to (1.1) should be preserved at the discrete level.

Note that the idea of relaxation methods for differential equations with third-order derivatives is to rewrite the original equation as a second-order differential system, and only then apply the finite volume method. The local auxiliary variables, introduced to approximate the derivatives of the solution, are superficial and can be easily removed for linear problems. A key ingredient for the success of such methods is the careful design of the cell interface numerical fluxes. All fluxes must be designed to guarantee stability and local solvability of the auxiliary variables. The obvious advantage of this approach is that the nonlinear equation (1.1) is transformed to a semilinear system (2.1) with linear characteristic variables easy to discretize without relying on Riemann problem solvers or iterative procedures.

The relaxation system (2.1) can be rewritten in vector form as

$$\mathbf{W}_t+\mathbf{A}\mathbf{W}_x=-\frac{1}{\varepsilon}\mathbf{Q}(\mathbf{W}),\tag{2.5}$$

where

$$\mathbf{W}=\begin{pmatrix} U\\ V\end{pmatrix},\qquad \mathbf{A}=\begin{pmatrix} 0 & 1\\ A & 0\end{pmatrix},\qquad \mathbf{Q}=\begin{pmatrix} 0\\ V-F(U)-\nu U_{xx}\end{pmatrix}.$$

Since the system (2.5) is hyperbolic, we can write $\mathbf{A}=\mathbf{R}\mathbf{\Lambda}\mathbf{R}^{-1}$, with $\mathbf{R}$ is the matrix of right eigenvectors of $\mathbf{A}$ and $\mathbf{\Lambda}$ is a diagonal matrix with eigenvalues of $\mathbf{A}$ as its elements. Their explicit expressions are given by

$$\mathbf{R}=\begin{pmatrix} 1 & 1\\ -\sqrt{A} & \sqrt{A}\end{pmatrix},\qquad \mathbf{R}^{-1}=\begin{pmatrix} \frac{1}{2} & -\frac{1}{2\sqrt{A}}\\ \frac{1}{2} & \frac{1}{2\sqrt{A}}\end{pmatrix},\qquad \mathbf{\Lambda}=\begin{pmatrix} -\sqrt{A} & 0\\ 0 & \sqrt{A}\end{pmatrix}.$$

To decouple Eq. (2.5) we introduce the characteristic variables $\mathbf{F}=\mathbf{R}^{-1}\mathbf{W}$. Therefore, Eq. (2.5) transforms to

$$\mathbf{F}_t+\mathbf{\Lambda}\mathbf{F}_x=-\frac{1}{\varepsilon}\mathbf{R}^{-1}\mathbf{Q}, \tag{2.6}$$

where

$$\mathbf{F}=\begin{pmatrix}\mathcal{F}\\ \mathcal{G}\end{pmatrix}=\mathbf{R}^{-1}\mathbf{W}=\begin{pmatrix}\frac{U}{2}-\frac{V}{2\sqrt{A}}\\ \frac{U}{2}+\frac{V}{2\sqrt{A}}\end{pmatrix},\qquad \mathbf{R}^{-1}\mathbf{Q}=\begin{pmatrix}\mathcal{F}-\hat{\mathcal{F}}\\ \mathcal{G}-\hat{\mathcal{G}}\end{pmatrix},$$

with $\hat{\mathcal{F}}$ and $\hat{\mathcal{G}}$ are the local equilibrium functions given by

$$\hat{\mathcal{F}}=\frac{U}{2}+\frac{F(U)}{2\sqrt{A}}+\frac{\nu}{2\sqrt{A}}U_{xx},\qquad \hat{\mathcal{G}}=\frac{U}{2}-\frac{F(U)}{2\sqrt{A}}-\frac{\nu}{2\sqrt{A}}U_{xx}.$$

Thus, we obtain an equivalent relaxation system in diagonalizable form

$$\begin{aligned}&\mathcal{F}_t+\sqrt{A}\mathcal{F}_x=-\frac{1}{\varepsilon}\left(\mathcal{F}-\hat{\mathcal{F}}\right),\\ &\mathcal{G}_t-\sqrt{A}\mathcal{G}_x=-\frac{1}{\varepsilon}\left(\mathcal{G}-\hat{\mathcal{G}}\right).\end{aligned} \tag{2.7}$$

It should be noted that in kinetic terminology, $\hat{\mathcal{F}}$ and $\hat{\mathcal{G}}$ are known by Maxwellians while, $\mathcal{F}$ and $\mathcal{G}$ are known by Riemann invariants and are related to the macroscopic variables $U$ and $V$ by

$$U=\mathcal{F}+\mathcal{G},\qquad V=\sqrt{A}(\mathcal{F}-\mathcal{G}). \tag{2.8}$$

It is easy to verify that the system (2.7) is strictly hyperbolic with two real distinct eigenvalues $\pm\sqrt{A}$ and linear characteristic variables given by

$$V\pm\sqrt{A}U. \tag{2.9}$$

We remark that the systems (2.7) and (2.1) are equivalent such that a discretization of each one of them leads essentially to the discretization of the other. In addition, for most of the examples solved in this paper, we assume periodic boundary conditions for both variables $U$ and $V$. This assumption is for simplicity in presentation only and is not essential. The method can be easily designed for nonperiodic boundary conditions. For instance, if Dirichlet boundary conditions are supplied for $U$ in (1.1) then the boundary conditions for the relaxation variable $V$ can be set to the local equilibrium (2.2), compare [3,10] for more discussions.

## 3 The finite volume method

The finite volume method is preferable in numerical solutions of partial differential equations due to its conservation properties. Standard relaxation methods have also been

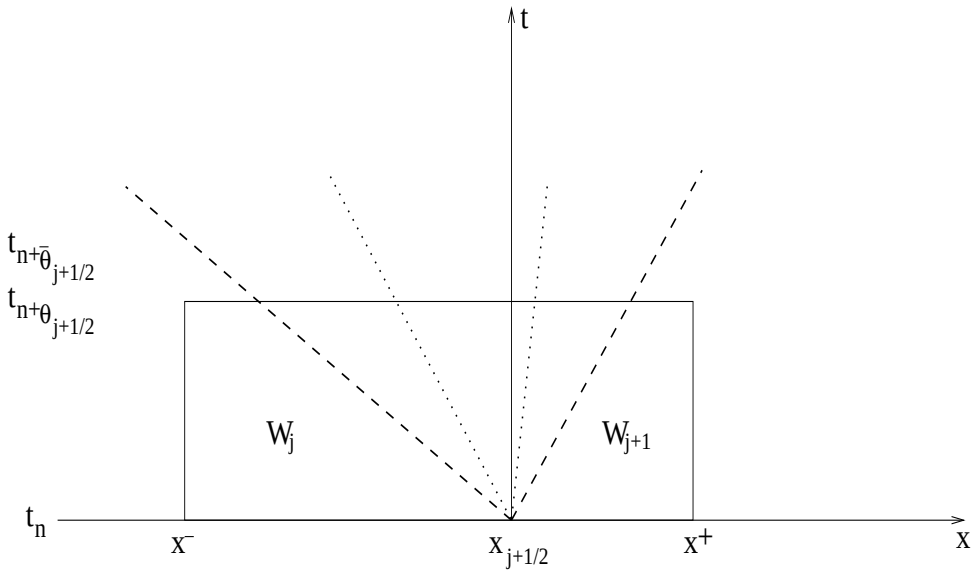


Figure 1: Illustration of the control space-time domain in finite-volume relaxation method. The dotted lines correspond to the original equation (1.1) and the dashed lines correspond to the relaxation system (2.1).

formulated in a finite-volume framework (see, for example [3, 10]). In this paper, we consider a new finite-volume relaxation method for the third-order differential equation (1.1). To formulate our method, we divide the spatial domain into $N$ computational cells $I_j=[x_{j-1/2},x_{j+1/2}]$ for $j=1,\cdots,N$. The center of the cell denoted by $x_j=(x_{j-1/2},x_{j+1/2})/2$ and the size of each cell by $\Delta x=x_{j+1/2}-x_{j-1/2}$. We denote by $\mathbf{W}_{j+1/2}$ the value of $\mathbf{W}$ at $x_{j+1/2}$ evaluated from the cell $I_{j+1}$. Integrating Eq. (2.5) over the space-time domain $]X^-,X^+[\times[t_n,t_{n+1}[$ shown in Fig. 1, we obtain

$$\int_{X^-}^{X^+}\mathbf{W}\left(x,t_n+\theta^n_{j+1/2}\right)dx=\mathbf{W}^n_j dX^-+\mathbf{W}^n_{j+1}dX^+-\theta^n_{j+1/2}\mathbf{A}^n_{j+1/2}\left(\mathbf{W}^n_{j+1}-\mathbf{W}^n_j\right)$$
$$-\frac{1}{\varepsilon}\int_{t_n}^{t_{n+1}}\int_{X^-}^{X^+}\mathbf{Q}(\mathbf{W})dxdt, \tag{3.1}$$

where the distances $dX^-$ and $dX^+$ are defined as $dX^\pm=\left|X^\pm-x_{j+1/2}\right|$. In (3.1), $\mathbf{W}^n_j$ denotes the space average of the solution $\mathbf{W}$ in the cell $]X^-,X^+[$ at time $t_n$

$$\mathbf{W}^n_j=\frac{1}{dX^-+dX^+}\int_{X^-}^{X^+}\mathbf{W}(x,t_n)dx.$$

We also define

$$\mathbf{W}^n_{j+1/2}=\frac{1}{dX^-+dX^+}\int_{X^-}^{X^+}\mathbf{W}(x,t_n+\theta^n_{j+1/2})dx. \tag{3.2}$$

The reconstruction of the numerical fluxes (3.2) is the essential step in most finite volume methods. The special structure of the nonlinear terms in (2.1) makes it trivial to evolve

the flux terms explicitly and the source term implicitly. To explain this feature, a simple implicit-explicit scheme applied to (2.1) yields

$$\begin{aligned}&\frac{U_j^{n+1}-U_j^n}{\Delta t}+\mathcal{D}_1 V_j^n=0,\\&\frac{V_j^{n+1}-V_j^n}{\Delta t}+A_{j+1/2}\mathcal{D}_1 U_j^n=-\frac{1}{\varepsilon}\Big(V_j^{n+1}-F(U_j^{n+1})-\nu\mathcal{D}_2 U_j^{n+1}\Big),\end{aligned}\tag{3.3}$$

where $\Delta t$ is the time stepsize, $\mathcal{D}_1 U_j^n$ and $\mathcal{D}_2 U_j^{n+1}$ denote the space discretization of the first-order and second-order differential operators,

$$\begin{aligned}&\mathcal{D}_1 U_j^n=\frac{U_{j+1/2}^n-U_{j-1/2}^n}{\Delta x},\\&\mathcal{D}_2 U_j^{n+1}=\frac{U_{j+1}^{n+1}-2U_j^{n+1}+U_{j-1}^{n+1}}{(\Delta x)^2}.\end{aligned}\tag{3.4}$$

Hence, the numerical solution $(U_j^{n+1},V_j^{n+1})$ is updated from (3.3) as

$$\begin{aligned}&U_j^{n+1}=U_j^n-\Delta t\Big(V_{j+1/2}^n-V_{j-1/2}^n\Big),\\&V_j^{n+1}=\frac{\varepsilon}{\varepsilon+\Delta t}\Big(V_j^n-\Delta t A_{j+1/2}\mathcal{D}_1 U_j^n\Big)+\frac{\Delta t}{\varepsilon+\Delta t}\Big(F(U_j^{n+1})+\nu\mathcal{D}_2 U_j^{n+1}\Big).\end{aligned}\tag{3.5}$$

Notice that the implicit-explicit scheme (3.5) avoids solution of linear or nonlinear systems. Furthermore, the scheme (3.5) is stable for all values of $\varepsilon$ (including $\varepsilon=0$) under the usual hyperbolic and parabolic CFL conditions. However, this scheme is only first-order accurate in time. In the current study we used a second-order implicit-explicit studied in [3,10,16]. Its implementation for Eq. (2.1) can be carried out using the following steps:

$$U_j^*=U_j^n,\tag{3.6a}$$

$$V_j^*=V_j^n+\frac{\Delta t}{\varepsilon}\Big(V_j^*-F(U_j^*)-\nu\mathcal{D}_2 U_j^*\Big);\tag{3.6b}$$

$$U_j^{(1)}=U_j^*-\Delta t\mathcal{D}_1 V_j^*,\tag{3.6c}$$

$$V_j^{(1)}=V_j^*-\Delta t A_{j+1/2}\mathcal{D}_1 U_j^*;\tag{3.6d}$$

$$U_j^{**}=U_j^{(1)},\tag{3.6e}$$

$$V_j^{**}=V_j^{(1)}-\frac{\Delta t}{\varepsilon}\Big(V_j^{**}-F(U_j^{**})-\nu\mathcal{D}_2 U_j^{**}\Big)-\frac{2\Delta t}{\varepsilon}\Big(V_j^*-F(U_j^*)-\nu\mathcal{D}_2 U_j^*\Big);\tag{3.6f}$$

$$U_j^{(2)}=U_j^{**}-\Delta t\mathcal{D}_1 V_j^{**},\quad V_j^{(2)}=V_j^{**}-\Delta t A_{j+1/2}\mathcal{D}_1 U_j^{**};\tag{3.6g}$$

$$U_j^{n+1}=\frac{1}{2}U_j^n+\frac{1}{2}U_j^{(2)},\quad V_j^{n+1}=\frac{1}{2}V_j^n+\frac{1}{2}V_j^{(2)}.\tag{3.6h}$$

Note that the time-discretization (3.6) in the limit when $\varepsilon \to 0$ converges to the formally TVD Runge-Kutta schemes given by Shu and Osher in [19], also referred to as Strong Stability-Preserving (SSP) time discretization methods in [8]. An accuracy study of this scheme is given in the Appendix for a linear case.

**Remark 3.1.** It is possible to construct an implicit-explicit scheme where the second-order differential term is treated implicitly in (3.6b) and (3.6f). By doing so, two linear systems of algebraic equations have to be solved at each time step during the time integration process. However, due to the extensive computational effort required for the linear solver, this may limit the efficiency of the relaxation scheme for solving Eq. (1.1).

The spatial discretization of the relaxation system (3.3) is complete when a numerical construction of $dX^-$, $dX^+$ and $\theta^n_{j+1/2}$ in (3.2) are chosen. A simple selection is $X^- = x_j$, $X^+ = x_{j+1}$ and $\theta^n_{j+1/2} = \alpha^n_{j+1/2}\Delta t/2$ with $\alpha^n_{j+1/2}$ is a positive parameter. This selection has been analyzed and experimented in [5] for conservation laws with source terms. In the present work, since the system (2.6) has linear characteristics, we can easily apply the finite-volume method for its discretization. Here, we set

$$\theta^n_{j+1/2} = \alpha^n_{j+1/2}\bar{\theta}_{j+1/2}, \qquad \bar{\theta}_{j+1/2} = \frac{\Delta x}{2S^n_{j+1/2}}, \qquad S^n_{j+1/2} = \max\left(\sqrt{A_j}, \sqrt{A_{j+1}}\right), \tag{3.7}$$

with $\sqrt{A_j}$ are the characteristic speeds in the relaxation system (2.6). Hence, the numerical fluxes required in the spatial discretization of (2.6) are defined as

$$\mathbf{F}^n_{j+1/2} = \frac{1}{2}\left(\mathbf{F}^n_j + \mathbf{F}^n_{j+1}\right) - \frac{\theta^n_{j+1/2}}{\Delta x}\mathbf{\Lambda}^n_{j+1/2}\left(\mathbf{F}^n_{j+1} - \mathbf{F}^n_j\right), \tag{3.8}$$

or equivalently

$$\begin{aligned} \mathcal{F}^n_{j+1/2} &= \frac{1}{2}\left(\mathcal{F}^n_j + \mathcal{F}^n_{j+1}\right) - \frac{\theta^n_{j+1/2}}{\Delta x}\sqrt{A^n_{j+1/2}}\left(\mathcal{F}^n_{j+1} - \mathcal{F}^n_j\right), \\ \mathcal{G}^n_{j+1/2} &= \frac{1}{2}\left(\mathcal{G}^n_j + \mathcal{G}^n_{j+1}\right) + \frac{\theta^n_{j+1/2}}{\Delta x}\sqrt{A^n_{j+1/2}}\left(\mathcal{G}^n_{j+1} - \mathcal{G}^n_j\right). \end{aligned} \tag{3.9}$$

Once $\mathcal{F}^n_{j+1/2}$ and $\mathcal{G}^n_{j+1/2}$ are reconstructed in (3.9), the numerical fluxes $U^n_{j+1/2}$ and $V^n_{j+1/2}$ in the relaxation system are obtained from (2.8) by

$$U_{j+1/2} = \mathcal{F}_{j+1/2} + \mathcal{G}_{j+1/2} \qquad \text{and} \qquad V_{j+1/2} = \sqrt{A_j}(\mathcal{F}_{j+1/2} - \mathcal{G}_{j+1/2}). \tag{3.10}$$

Clearly, the accuracy of the finite volume method will depend on the choice of the characteristic speeds $\sqrt{A_{j+1/2}}$ in (3.9). A simple selection can be based on rough estimates of eigenvalues of $F'(U)$ as $\sqrt{A^n_{j+1/2}} = \mathcal{A}$ with $\mathcal{A}$ is a positive constant satisfying

$$\mathcal{A} \geq \left|F'(U)\right|. \tag{3.11}$$

Other choice is to calculate $\sqrt{A_j}$ locally at each control volume as

$$\sqrt{A^n_{j+1/2}}=\max\Big\{\big|F'(U^n_j)\big|,\big|F'(U^n_{j+1})\big|\Big\}. \tag{3.12}$$

A global choice is to take the maximum over the gridpoints in (3.12). It is worth saying that, larger values of $\sqrt{A^n_{j+1/2}}$ usually add more numerical dissipation. For a discussion on the role of the characteristic speeds in relaxation schemes we refer the reader to our previous works [3,18] and the references are therein.

**Remark 3.2.** Some remarks are in order:

• The relaxation rate $\varepsilon$ can be viewed as a viscosity coefficient in (2.1) such that more numerical diffusion is added for larger value of $\varepsilon$. For small $\varepsilon$, numerical results obtained by relaxing scheme ($\varepsilon\ll 1$) and relaxed scheme ($\varepsilon=0$) are essentially the same.

• The slopes $S^n_{j+1/2}$ in (3.7) can be viewed as the Rusanov speeds. By letting $\alpha^n_{j+1/2}=1$ the spatial discretization (3.9) leads to the well-established Lax-Wendroff scheme. For homogeneous systems, the reconstruction (3.9) is exactly the VFRoe scheme studied in [13]. Another selection of $\alpha^n_{j+1/2}$ based on sign matrix has been investigated in [15].

• Using constant characteristic speeds satisfying (3.11), the discretization (3.9) gives

$$\begin{aligned}
\mathcal{F}^n_{j+1/2}&=\frac{1}{2}\Big(\mathcal{F}^n_j+\mathcal{F}^n_{j+1}\Big)-\frac{\alpha^n_{j+1/2}}{2}\Big(\mathcal{F}^n_{j+1}-\mathcal{F}^n_j\Big),\\
\mathcal{G}^n_{j+1/2}&=\frac{1}{2}\Big(\mathcal{G}^n_j+\mathcal{G}^n_{j+1}\Big)+\frac{\alpha^n_{j+1/2}}{2}\Big(\mathcal{G}^n_{j+1}-\mathcal{G}^n_j\Big).
\end{aligned} \tag{3.13}$$

To obtain the numerical fluxes in (3.3) one solves (3.13) and (3.10) as

$$\begin{aligned}
U^n_{j+1/2}&=\frac{1}{2}\Big(U^n_{j+1}+U^n_j\Big)-\frac{\alpha^n_{j+1/2}}{2\mathcal{A}}\Big(V^n_{j+1}-V^n_j\Big),\\
V^n_{j+1/2}&=\frac{1}{2}\Big(V^n_{j+1}+V^n_j\Big)-\frac{\alpha^n_{j+1/2}}{2}\mathcal{A}\Big(U^n_{j+1}-U^n_j\Big).
\end{aligned} \tag{3.14}$$

Again, if $\alpha^n_{j+1/2}=1$ the reconstruction (3.13) reduces to the first-order upwinding

$$\mathcal{F}^n_{j+1/2}=\mathcal{F}^n_j \qquad \text{and} \qquad \mathcal{G}^n_{j+1/2}=\mathcal{G}^n_{j+1}. \tag{3.15}$$

Notice that the upwind scheme (3.15) was early used in [10,16]. It is worth remarking that the results presented in section 4 were obtained using uniform meshes. However, our reconstruction can be applied for unstructured meshes without major conceptual modifications.

Another choice of the slopes $\alpha^n_{j+1/2}$ leading to a first-order scheme is $\alpha^n_{j+1/2}=\tilde{\alpha}^n_{j+1/2}$ where

$$\tilde{\alpha}^n_{j+1/2}=S^n_{j+1/2}/s^n_{j+1/2}, \tag{3.16}$$

with

$$S^n_{j+1/2}=\max\left(\sqrt{A_j},\sqrt{A_{j+1}}\right) \qquad \text{and} \qquad s^n_{j+1/2}=\min\left(\sqrt{A_j},\sqrt{A_{j+1}}\right).$$

Moreover, if constant characteristic speeds are used then, $\tilde{\alpha}^n_{j+1/2}=1$ and the scheme results in the first-order upwinding (3.15). In the present work, we consider a second-order scheme incorporating limiters in its reconstruction as

$$\alpha^n_{j+1/2}=\tilde{\alpha}^n_{j+1/2}+\sigma^n_{j+1/2}\Psi\left(r_j\right), \tag{3.17}$$

where $\tilde{\alpha}^n_{j+1/2}$ is given by (3.16) and

$$\sigma^n_{j+1/2}=\frac{\Delta t}{\Delta x}S^n_{j+1/2}-\frac{S^n_{j+1/2}}{s^n_{j+1/2}}, \qquad r_j=\frac{\mathcal{F}^n_j-\mathcal{F}^n_{j-1}}{\mathcal{F}^n_{j+1}-\mathcal{F}^n_j}.$$

The reconstruction for the variable $\mathcal{G}$ is performed in similar manner. In (3.17), $\Psi(r)$ defines the van Leer slope limiter function [20], $\Psi(r)=(|r|+r)/(1+|r|)$. Note that other slope limiter functions such Minmod or Superbee functions can also apply. The reconstructed slopes (3.17) are inserted in (3.7)-(3.9) and the numerical fluxes $U^n_{j+1/2}$ and $V^n_{j+1/2}$ are computed from (3.10). Remark that if we set $\Psi=0$, the spatial discretization (3.17) reduces to the first-order scheme.

## 4 Numerical examples

In this section we present few numerical examples to demonstrate the accuracy and capacity of the relaxation finite-volume method described in the previous sections. In all these examples we solve the KdV equation

$$\begin{aligned} &U_t+\left(U^2\right)_x+\nu U_{xxx}=0, \qquad (x,t)\in[-M,M]\times(0,T],\\ &U(x,0)=\bar{U}(x), \qquad x\in[-M,M]. \end{aligned} \tag{4.1}$$

This equation which was developed for nonlinear shallow water waves, has been found relevant in other physical models such as ion acoustic waves in a plasma and acoustic waves in an harmonic crystal, see for example [7, 9, 11]. In addition, the KdV equation is a natural test problem for comparing conservative versus dissipative discretizations in numerical schemes for dispersive equations.

Note that, since in most of the examples considered in this section, $U(x,t)$ converges to 0 exponentially as $|x|\to\infty$, the initial value problem (1.1) is approximated by an initial-boundary value problem for $x\in[-M,M]$ as long as the soliton does not reach the boundaries. We choose a suitable $M$ to fit in with different examples. The relaxation system associated with Eq. (4.1) is reconstructed as in (2.1). In all our computations the characteristic speeds $A$ are calculated locally at each control volume as

$$\sqrt{A_{j+1/2}}=\max\left\{\left|U_j\right|,\left|U_{j+1}\right|\right\}. \tag{4.2}$$

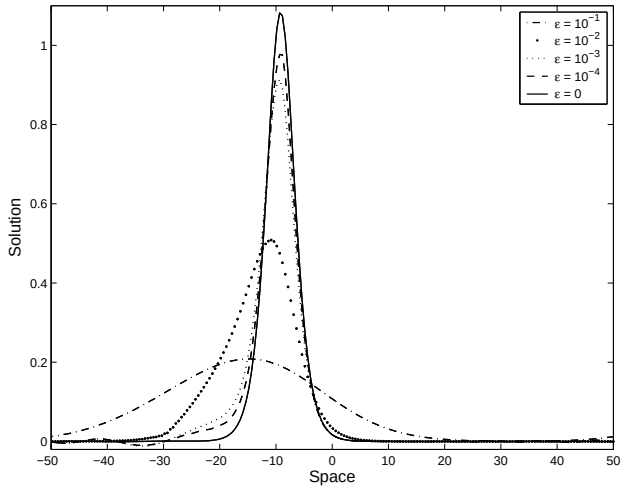


Figure 2: Asymptotic-preserving plots for the single solitary wave at $t=30$.

Other selection of characteristic speeds in general relaxation methods have been discussed in references [3, 17, 18]. Moreover, the courant number $C$ is fixed to 0.5 and we use variable time stepsizes $\Delta t$ adjusted at each time step according to the condition

$$\Delta t = C\min\left(\frac{\Delta x}{\max_j\left(\sqrt{A_{j+1/2}}\right)},\frac{(\Delta x)^2}{\nu}\right),$$

We present numerical results for the following soliton examples of the KdV equation.

### 4.1 Single solitary wave

As a first example we solve the KdV equation (4.1) for a single soliton with known analytical solution given by

$$U(x,t)=12\nu c^2\,\mathrm{sech}^2\left(c(x-4\nu c^2 t-x_0)\right), \tag{4.3}$$

where $M=50$ and

$$c=0.3, \qquad x_0=-20.$$

The initial condition $\bar{U}(x)$ is calculated from the exact solution (4.3). For boundary conditions $U(-M,t)$, $U(M,t)$ and $U_x(M,t)$, we simply use the values extracted from the exact solution. The boundary conditions $V(-M,t)$, $V(M,t)$ and $V_x(M,t)$ are obtained according to the local equilibrium (2.2). This example is served to check the accuracy of the finite-volume relaxation method for dispersive equations. First, we examine the asymptotic-preserving property of the relaxation method. To this end we display in Fig. 2 the obtained solutions for different relaxation rates $\varepsilon$ at time $t=30$ using $\nu=1$ and 200 cells. We observe that for large values of $\varepsilon$ the computed solution is far from the correct

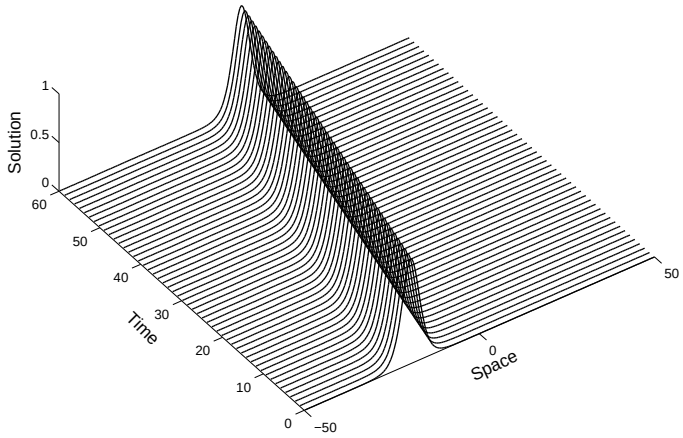


Figure 3: Single solitary wave.

Table 1: Relative errors for the single solitary wave at $t=30$ and two different values of $\nu$.

| | $\nu=0.001$ | | | | $\nu=1$ | | | |
|---|---|---|---|---|---|---|---|---|
| $N$ | $L^2$-error | Rate | $L^\infty$-error | Rate | $L^2$-error | Rate | $L^\infty$-error | Rate |
| 50 | 5.103195$E$-4 | — | 5.149129$E$-4 | — | 1.381533$E$-1 | — | 1.012682$E$-1 | — |
| 100 | 1.559843$E$-4 | 1.71 | 1.640719$E$-4 | 1.65 | 3.779509$E$-2 | 1.87 | 2.888078$E$-2 | 1.81 |
| 200 | 4.479472$E$-5 | 1.80 | 4.775029$E$-5 | 1.78 | 9.514495$E$-3 | 1.99 | 7.270416$E$-3 | 1.99 |
| 400 | 1.127657$E$-5 | 1.99 | 1.202683$E$-5 | 1.99 | 2.173661$E$-3 | 2.13 | 1.684170$E$-3 | 2.11 |
| 800 | 2.612184$E$-6 | 2.11 | 2.844519$E$-6 | 2.08 | 4.698027$E$-4 | 2.21 | 3.690883$E$-4 | 2.19 |

limit solution. Decreasing the relaxation rate results in an improvement of the computed solution. For $\varepsilon=0$, the computed solution and the exact solution coincide. This confirms the formal convergence analysis of relaxation system to the original conservation law as $\varepsilon\to 0$. Furthermore, these results show that the finite-volume discretization maintains the correct asymptotic limit.

In Fig. 3 we plot the evolution of the soliton in the time-space domain. Note the single soliton (4.3) propagates to the right with speed $c=0.3$. This motion has been well captured by our method without diffusing the soliton profile or introducing nonphysical oscillations.

Our next concern is to perform a convergence study for the finite-volume relaxation method. The relative $L^2$ and $L^\infty$ errors are listed in Table 1 for the single solitary wave at $t=30$ using two different values of the dispersion coefficient $\nu$ and $\varepsilon=0$. All the errors are measured by the difference between the pointvalues of the exact solution (4.3) and the reconstructed pointvalues of the computed solution. As expected, for the two selected dispersion coefficients, the errors decay as the number of gridpoints $N$ increases. A slow decay rate has been detected in the errors for $\nu=1$. We can clearly see that the finite-

volume relaxation scheme shows a second-order accuracy in space for the considered single solitary wave.

In what follows we present results only for the relaxed computations ($\varepsilon=0$) and the KdV equation is solved subject to periodic boundary conditions. In addition, the computational domain is discretized into 200 control volumes and the dispersion coefficient $\nu=1$ in all the computations.

### 4.2 Interaction of three solitons

Next we solve a three solitary waves characterized by Eq. (4.1) subject to the following initial condition

$$\bar{U}(x)=\sum_{i=1}^{3}12c_i^2\text{sech}^2\left(c_i(x-x_i)\right), \tag{4.4}$$

where $M=90$ and

$$c_1=0.3,\quad c_2=0.25,\quad c_3=0.2,\quad x_1=-60,\quad x_2=-44,\quad x_3=-26.$$

The obtained result is displayed in Fig. 4. As can be seen the three pulses travel with time to the right. But the taller soliton moves faster, hence the three occasionally merge and then split apart again. The relaxation method captures accurately the evolution of the solitons in the computational domain without diffusing the fronts neither introducing oscillations near steep gradients. Our finite-volume relaxation method performs well for this test example. Note that the performance of our method is very attractive since the computed solution remains, stable, monotone and highly accurate even on coarse meshes without solving Riemann problems or requiring special front tracking procedures.

### 4.3 Interaction of four solitons

In this example we study the interaction of four solitary waves defined by the initial condition

$$\bar{U}(x)=\sum_{i=1}^{4}12c_i^2\text{sech}^2\left(c_i(x-x_i)\right), \tag{4.5}$$

where $M=120$ and

$$\begin{aligned}&c_1=0.3,\quad c_2=0.25,\quad c_3=0.2,\quad c_4=0.15,\\&x_1=-85,\quad x_2=-60,\quad x_3=-35,\quad x_4=-10.\end{aligned}$$

Fig. 5 depicts the evolution of the computed solution in the time-space phase. We observe that the soliton with higher amplitude moves with faster speed, and the amplitudes of the five waves are well preserved at the final time of computation. This indicates that our finite-volume relaxation method has an excellent conservation property. Furthermore, the resolution achieved by the new finite-volume relaxation method agree well with most of the results obtained by typical non-dissipative schemes for the dispersive equations.

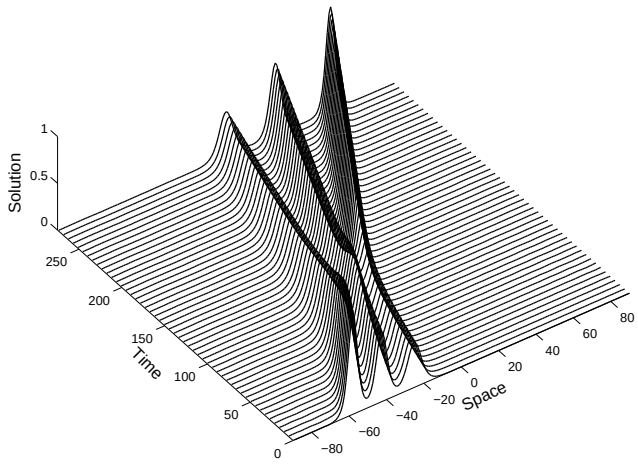


Figure 4: Solitary wave interaction of three solitons.

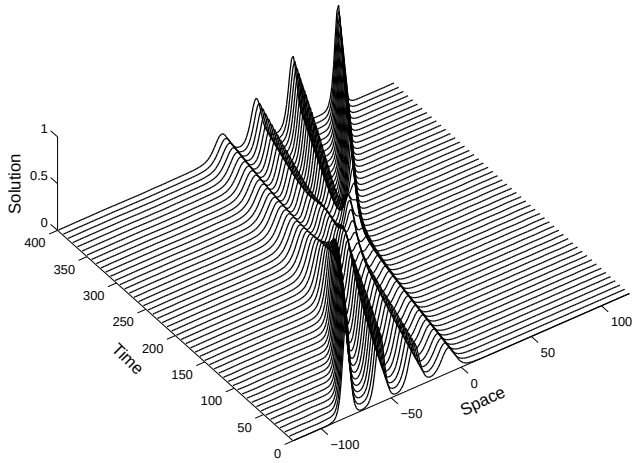


Figure 5: Solitary wave interaction of four solitons.

## 4.4 Interaction of five solitons

Our last example solves the KdV equation for a five solitons splitting. This test case has the initial condition

$$\bar{U}(x)=\sum_{i=1}^{5}12c_i^2\mathrm{sech}^2\left(c_i(x-x_i)\right), \tag{4.6}$$

where $M=150$ and

$$c_1=0.3,\quad c_2=0.25,\quad c_3=0.2,\quad c_4=0.15,\quad c_5=0.1,$$
$$x_1=-120,\quad x_2=-90,\quad x_3=-60,\quad x_4=-30,\quad x_5=0.$$

In Fig. 6 we show the obtained results for Eqs. (4.1) and (4.6). The solution is completely free of spurious oscillations and no extensive numerical dissipation is detected. The re-

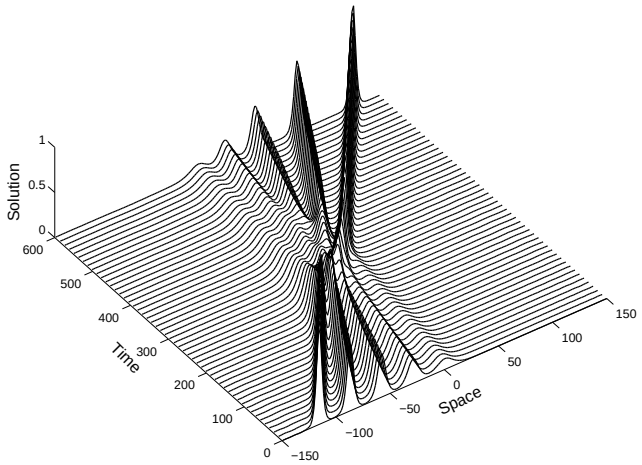


Figure 6: Solitary wave interaction of five solitons.

sults again indicate very good performance of the finite-volume relaxation method for this test example. We can see the small complex structures of the solitons being captured by the proposed method. Clearly our method is very suitable for computing such solutions.

## 5 Conclusions

We have proposed new finite-volume relaxation methods for the third-order differential equations. The relaxation approximation and a finite volume method have been successfully combined and turned into a second-order scheme to tackle some difficulties in the numerical integration of the nonlinear dispersive equations. Numerical simulations for the Korteweg-de Vires equation, as prototypical test case for third-order differential equations, have been presented for different wave patterns. Our numerical results indicate that the proposed method is extremely accurate and efficient and most suitable for the study of complex dynamics of higher-order equations. Our relaxation scheme resolves these problems accurately and captures the long wave behavior without using eigenvector decompositions or Riemann solvers.

High-order discretizations which have non-oscillatory solvers maintaining the local structure of the method, and accuracy enhancement study, and more numerical experiments with physically interesting two-dimensional problems constitute an ongoing work.

## Acknowledgments

Part of this work was performed during a visit of the second author to the Université Paris 13. M. Seaïd would like to thank Department of Mathematics at Université Paris 13 for their hospitality and for technical and financial support.

## Appendix: Accuracy study of the implicit-explicit scheme

In this appendix we perform an accuracy study for the implicit-explicit scheme (3.6) for the relaxation system (2.1). Let us first rewrite the system (2.1) in the general ODE form

$$\frac{d\mathbf{U}}{dt}+H(\mathbf{U})=-\frac{1}{\varepsilon}S(\mathbf{U}). \tag{A.1}$$

Then we apply the implicit-explicit scheme (3.6) to the system (A.1) for the linear case $H(\mathbf{U})=\Lambda\mathbf{U}$ and $S(\mathbf{U})=\Gamma\mathbf{U}$, with $\Lambda$ and $\Gamma$ are constant matrices. If we further set $\varepsilon=1$, the scheme (3.6) reduces to

$$\mathbf{U}^*=\mathbf{U}^n+\Gamma\Delta t\mathbf{U}^*, \tag{A.2a}$$
$$\mathbf{U}^{(1)}=\mathbf{U}^*-\Lambda\Delta t\mathbf{U}^*, \tag{A.2b}$$
$$\mathbf{U}^{**}=\mathbf{U}^{(1)}-\Gamma\Delta t\mathbf{U}^{**}-2\Gamma\Delta t\mathbf{U}^*, \tag{A.2c}$$
$$\mathbf{U}^{(2)}=\mathbf{U}^{**}-\Lambda\Delta t\mathbf{U}^{**}, \tag{A.2d}$$
$$\mathbf{U}^{n+1}=\frac{1}{2}\mathbf{U}^n+\frac{1}{2}\mathbf{U}^{(2)}. \tag{A.2e}$$

It is easy to verify that the exact solution of (A.1) in the interval $[n\Delta t,(n+1)\Delta t]$ is given by

$$\mathbf{U}^{n+1}=e^{-(\Lambda+\Gamma)\Delta t}\mathbf{U}^n, \tag{A.3}$$

Let us also assume that $\|\Lambda\|\Delta t<1$ and $2\|\Gamma\|\Delta t<1$ such that the matrices in (A.2) are invertible. Hence, Eq. (A.2) can be rewritten as

$$\mathbf{U}^*=(\mathbf{I}-\Gamma\Delta t)^{-1}\mathbf{U}^n, \tag{A.4a}$$
$$\mathbf{U}^{(1)}=(\mathbf{I}-\Lambda\Delta t)(\mathbf{I}-\Gamma\Delta t)^{-1}\mathbf{U}^n, \tag{A.4b}$$
$$\mathbf{U}^{**}=(\mathbf{I}+\Gamma\Delta t)^{-1}\left(\mathbf{U}^{(1)}-2\Gamma\Delta t\mathbf{U}^*\right), \tag{A.4c}$$
$$\mathbf{U}^{(2)}=(\mathbf{I}-\Lambda\Delta t)\mathbf{U}^{**}, \tag{A.4d}$$
$$\mathbf{U}^{n+1}=\frac{1}{2}\mathbf{U}^n+\frac{1}{2}\mathbf{U}^{(2)}, \tag{A.4e}$$

where $\mathbf{I}$ denotes the identity matrix. Expanding Eqs. (A.4a) and (A.4b) up to the order $\mathcal{O}(\Delta t^3)$, we obtain

$$\mathbf{U}^*=\left(\mathbf{I}+\Gamma\Delta t+\Gamma^2\Delta t^2\right)\mathbf{U}^n+\mathcal{O}(\Delta t^3), \tag{A.5}$$
$$\mathbf{U}^{(1)}=\left(\mathbf{I}+(\Gamma-\Lambda)\Delta t+(\Gamma^2-\Lambda\Gamma)\Delta t^2\right)\mathbf{U}^n+\mathcal{O}(\Delta t^3), \tag{A.6}$$

Next, we substitute (A.5) and (A.6) into (A.4c) and results

$$\mathbf{U}^{**}=\left(\mathbf{I}-(2\Gamma+\Lambda)\Delta t+\Gamma^2\Delta t^2\right)\mathbf{U}^n+\mathcal{O}(\Delta t^3). \tag{A.7}$$

Combining (A.7) and (A.4d) one obtains

$$\mathbf{U}^{(2)}=\Big(\mathbf{I}-(2\Gamma+2\Lambda)\Delta t+\big(\Gamma^2+2\Lambda\Gamma+\Lambda^2\big)\Delta t^2\Big)\mathbf{U}^n+\mathcal{O}\left(\Delta t^3\right). \tag{A.8}$$

Finally, substituting (A.8) into (A.4e) we obtain

$$\begin{aligned}\mathbf{U}^{n+1}&=\Big(\mathbf{I}-(\Gamma+\Lambda)+\frac{1}{2}(\Gamma+\Lambda)^2\Big)\mathbf{U}^n+\mathcal{O}\left(\Delta t^3\right),\\&=e^{-(\Lambda+\Gamma)\Delta t}\mathbf{U}^n+\mathcal{O}\left(\Delta t^3\right).\end{aligned} \tag{A.9}$$

This shows a second-order accuracy for the implicit-explicit scheme (3.6) applied to the ODE (A.1).

## References


[1] F. Alcrudo and F. Benkhaldoun, Exact solutions to the Riemann problem of the shallow water equations with a bottom step, Comput. Fluids, **30**, 643–671 (2001).

[2] M. Banda and M. Seaïd, Nonoscillatory methods for relaxation approximation of Hamilton-Jacobi equations, Appl. Math. Comput., **183**, 170–183 (2006).

[3] M. Banda and M. Seaïd, Higher-Order relaxation schemes for hyperbolic systems of conservation laws, Numer. Math., **26**, 999–1017 (1995).

[4] T.B. Benjamin, J.L. Bona and J.J. Mahony, Model equations for long waves in nonlinear, dispersive systems, Phil. Trans. Roy. Soc. London Ser. A., **272**, 47–78 (1972).

[5] F. Benkhaldoun, Analysis and validation of a new finite volume scheme for nonhomogeneous systems, Finite Volumes for Complex Applications III., 269–276 (2002).

[6] F. Cavalli, G. Naldi, G. Puppo and M. Semplice, High-order relaxation schemes for nonlinear degenerate diffusion problems, SIAM J. Numer. Anal., **45**, 2098–2119 (2007).

[7] P.G. Drazin and R.S. Johnson, Solitons: An Introduction, Cambridge University Press, 1989.

[8] S. Gottlieb, C.W. Shu and E. Tadmor, Strong stability-preserving high-order time discretisation methods, SIAM Rev., **43**, 89–112 (2001).

[9] E. Infeld and G. Rowlands, Nonlinear Waves, Solitons and Chaos, Cambridge University Press, 2000.

[10] S. Jin and Z. Xin, The relaxation schemes for systems of conservation laws in arbitrary space dimensions, Comm. Pure Appl. Math., **48**, 235–277 (1995).

[11] D.J. Korteweg and G. de Vries, On the change of form of long waves advecting in a rectangular canal and on a new type of long stationary waves, Philos. Mag., **39**, 422–443 (1895).

[12] G.L. Lamb, Elements of Soliton Theory, John Wiley, New York 1980.

[13] J.M. Masella, I. Faille and T. Gallouët, On an approximate Godunov scheme, Int. J. Comp. Fluids Dynamics., **13**, 133–149 (1999).

[14] G. Naldi and L. Pareschi, Numerical schemes for hyperbolic systems of conservation laws with stiff diffusie relaxation, SIAM J. Numer. Anal., **37**, 1246–1270 (2000).

[15] S. Sahmim, F. Benkhaldoun and F. Alcrudo, A finite volume solver based on matrix sign for nonhomogeneous systems, Finite Volumes for Complex Applications IV., 471–482 (2005).

[16] M. Seaïd, Stable numerical methods for conservation laws with discontinuous flux function, Appl. Math. Comput., **175**, 383-400 (2006).

[17] M. Seaïd, High-resolution relaxation scheme for the two-dimensional Riemann problems in gas dynamics, Numer. Meth. Part. Diff. Eq., **22**, 397–413 (2006).

[18] M. Seaïd, Non-oscillatory relaxation methods for the shallow water equations in one and two space dimensions, Int. J. Num. Meth. Fluids., **46**, 457–484 (2004).
[19] C.W. Shu and S. Osher, Efficient implementation of essentially non-oscillatory shock-capturing schemes, J. Comput. Phys., **77**, 439–471 (1988).
[20] B. Van Leer, Towards the ultimate conservative difference schemes V. A second-order sequal to Godunov's method, J. Comput. Phys., **32**, 101–136 (1979).